

# Run-and-tumble in a crowded environment: persistent exclusion process for swimmers

Rodrigo Soto<sup>1,2</sup> and Ramin Golestanian<sup>2</sup>

<sup>1</sup>*Departamento de Física, Facultad de Ciencias Físicas y Matemáticas  
Universidad de Chile, Av. Blanco Encalada 2008, Santiago, Chile*

<sup>2</sup>*Rudolf Peierls Centre for Theoretical Physics, University of Oxford, Oxford OX1 3NP, UK  
(Dated: June 6, 2019)*

The effect of crowding on the run-and-tumble dynamics of swimmers such as bacteria is studied using a discrete lattice model of mutually excluding particles that move with constant velocity along a direction that is randomized at a rate  $\alpha$ . In stationary state, the system is found to break into dense clusters of a characteristic size that predominantly scales as  $\alpha^{-0.5}$ , in which particles are trapped or stopped from moving for a time of order  $\alpha^{-1.7}$  for a range of densities, due to cooperative effects. Our findings might be helpful in understanding the early stages of biofilm formation.

PACS numbers: 87.10.Mn, 05.50.+q, 87.17.Jj

Bacterial biofilms are fascinating examples of biological development into multicellular communities through aggregation [1], and exhibit novel properties such as differentiation and delegation of function [2]. A prominent feature of biofilms, which poses a challenge for treatment of diseases caused by some pathogens, is that the bacteria inhabiting them are phenotypically different from their free-swimming counterparts [3]. For example, when individual bacteria interact with surfaces, they undergo transformations that help them adapt to the new conditions by adopting different modes of motility [4]. A biofilm nucleation could form when a number of bacteria decide to settle down near a surface and become completely localized. In addition to environmental cues, a key factor in triggering such phenotypic transformations for individual bacteria is the time they spend in any given neighborhood and under the influence of the corresponding local conditions; a factor that could be strongly influenced by *crowding*. If they happen to be stuck in a place for a certain amount of time, they decide to adapt to the new lifestyle by converting into the appropriate phenotype. Therefore, a natural question arises from a physics viewpoint: what is the time motile bacteria could spend being held up in their own traffic jams near a surface?

Self-propelled particles with excluded volume have been shown to develop jammed regions even at low global concentrations when they have a local alignment interaction [5]. It has been argued that such density patterns could form due to effective mobility reduction in the presence of nearby swimmers [6, 7]. This reduction has been experimentally characterized by measuring the self-diffusion process [8]. Using a coarse-grained description of the swimmer dynamics and considering a mean-field approximation for the mobility reduction, it has been shown that the system phase separates into dense and dilute regions via a spinodal decomposition with long-time coarsening [7]. If local ferromagnetic alignment is included, jammed clusters of macroscopic size with internal grain boundaries are formed [9].

Here, we present a lattice model that mimics the bacte-

rial run-and-tumble dynamics by allowing the particles to have a persistent motion, and incorporates excluded volume by only allowing single occupancy for each site. Our model of the resulting persistent exclusion process (PEP) is a lattice implementation of the continuous model presented in Refs. [7, 10, 11]. For a wide range of particle concentrations and tumbling rates the PEP generates clusters of jammed particles, separated by dilute regions with moving particles. We probe the stationary distribution and the characteristic size of the clusters, the statistics of the stopping time for individual particles, and the reduction in the average number of moving particles due to jamming, as functions of the concentration and the tumbling rate. We find novel universal scaling behaviors, and a counterintuitive effective superdiffusive behavior of the particles inside the jammed clusters.

We consider a one dimensional (1D) lattice consisting of  $N$  sites, where each site can be occupied by at most one particle. To model the persistent motion in the run phase, particles are characterized by a label that indicates the direction they move: left or right. The (dimensionless) particle concentration is  $\phi$  and  $M = \phi N$  is the total number of particles. At each time step  $M$  particles are chosen sequentially at random. For each particle, a new direction is chosen at random with probability  $\alpha$  to model the tumble events; otherwise it preserves the previous direction. At this stage, if the neighboring site as pointed by the director is empty, it will move to this new position. The evolution of the model is asynchronous (sequential update) and stochastic. Periodic boundary conditions are used and units are chosen such that the lattice spacing and the time step are fixed to unity. Particles are initially placed at random mutually excluding positions and each particle is assigned a random direction.

It is important to first highlight the key differences between the PEP model and other similar models proposed to describe swimmers, and to examine its behavior in certain limiting cases. Our model does not include the ferromagnetic interaction as in Ref. [9], and the direction after

tumbling is random. In Ref. [12] the hopping probability to occupied sites is gradually decreased when the site density is increased, whereas here excluded volume is strictly enforced at each site. Our model is related to other lattice models used to describe nonequilibrium behavior, in certain limits. When  $\alpha = 1$ , the particles are reoriented at each time step and no persistent motion is obtained. This corresponds to the symmetric exclusion process (SEP), for which many exact properties are known [13, 14]. In particular, SEP is an equilibrium process with vanishing static spatial correlations among sites, implying that the fraction of moving particles  $\mu$  equals the fraction of empty sites, i.e.  $\mu = 1 - \phi$ . The asymmetric exclusion process (ASEP) is a nonequilibrium process that breaks the detailed-balance by breaking the spatial symmetry, resulting in a directed flux [15, 16]. This process and the totally asymmetric exclusion process (TASEP) show interesting nonequilibrium properties that result from the particle interactions [15–20]. In the PEP, the nonequilibrium feature is introduced via the persistent motion that is controlled by  $\alpha$ ; a property that is absent in the ASEP and TASEP cases. If the limit of infinite dilution, each particle moves in straight-line run-segments for periods of time that are geometrically distributed with the average of  $\alpha^{-1}$ , followed by a complete reorientation (tumble). Consequently, at time scales longer than  $\alpha^{-1}$ , each particle performs a random walk with an effective diffusion coefficient of  $D_1 = \alpha^{-1}$  [21]. At finite concentrations, cooperative effects appear, which are the main interest of this Letter.

When  $\alpha = 0$  the system evolves to an absorbing state in which the particles are all jammed. Jamming is produced by a particle that moves in a given direction and meets another particle that has the opposite direction, remaining blocked as a cluster seed. Moving particles are absorbed into the existing clusters until no isolated particles remain. At finite values of  $\alpha$  the system shows the formation of clusters that coexist with dilute regions. This is a dynamic state as the particles at the borders of the clusters can evaporate. The evaporation rate is  $\alpha/2$  as only half of the tumbling processes are effective in pointing into the escape direction. The cluster dynamics involves three types of processes: formation by the collision of two oppositely moving particles, absorption of moving particles at the border, and evaporation at the boundaries. No merging or splitting processes are possible as the clusters are immobile.

We present results obtained in the stationary regime of simulations with  $N = 2000$  sites, spanning the parameter range  $0.01 \leq \phi \leq 0.9$  and  $0.001 \leq \alpha \leq 1$ , and total simulation time of  $T_{\max} = 10^7$ . Figure 1 presents spatiotemporal diagrams of the system. At each time step, the system is clearly separated into dense clusters and dilute regions (denoted here as gas), which alternate. Gas regions contain none or some isolated moving particles. Clusters, on the contrary, are close packed

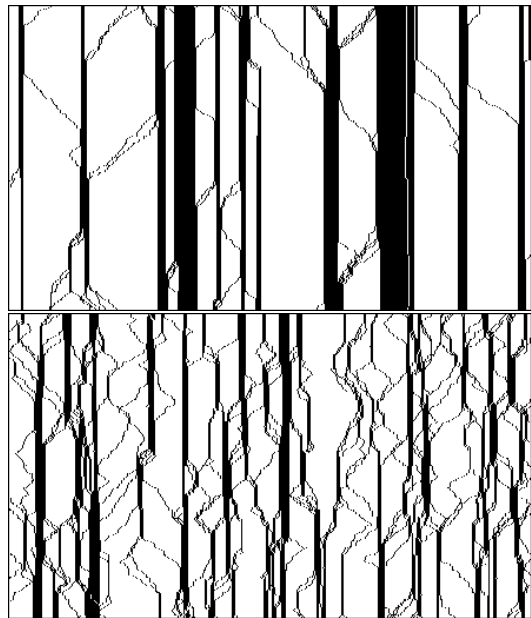


FIG. 1. Spatiotemporal plot with  $N = 2000$ ,  $\phi = 0.2$ , and  $\alpha = 0.01$  (top) and  $\alpha = 0.05$  (bottom). For clarity, only a fraction of the system  $0 \leq x \leq 500$  is shown for a time window of  $T = 300$  in the stationary regime, with the time increasing upwards. The particles are shown as black dots. In the gas phase, they move with unit average velocity but their trajectory is fluctuating as a consequence of the dynamics being stochastic.

( $\phi_c = 1$ ), with the particle on the left (right) border pointing to the right (left). The interior particles have a distribution of orientations as a result of successive reorientations they experience. This internal structure of the clusters explains why we can observe rapid emission of two or more particles in the figure. When a border particle tumbles, the neighboring particle could be pointing outward with probability  $1/2$ , and thus the two could be emitted together in successive time steps. More particles could follow with decreasing probabilities, but on average two particles will be emitted in each evaporation process.

We can argue that the above picture holds when  $\alpha < \phi$ . If  $\phi_g$  denotes the average particle concentration in the gas phase, the cluster absorbs a gas particle at a rate  $\phi_g/2$ . Dynamic equilibrium is reached when  $\phi_g = \alpha$ , since the evaporation rate is  $\alpha/2$ . Therefore, the cluster sizes are adjusted by the equilibration with the gas phase. The described picture can only be valid if  $\phi_g < \phi$ , i.e. if  $\alpha < \phi$ . The above simple kinetic picture for the dynamic equilibrium when  $\alpha \ll \phi$  undergoes a diffusive motion with diffusion coefficient  $D_b = \alpha$ . This is to be contrasted with the single particle diffusion coefficient  $D_1 = \alpha^{-1}$ . In the opposite case of  $\alpha > \phi$ , the dynamics is no longer only via the motion of the cluster boundaries, and we must consider the internal dynamics of the gas phase.

We find that in the stationary state the cluster sizes

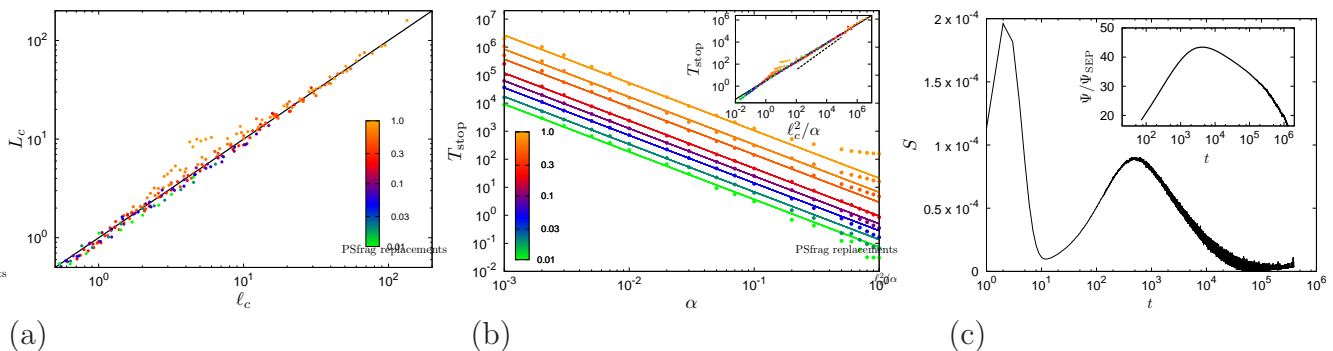


FIG. 2. (color online.) (a) Data collapse plot for the average cluster size  $L_c$  as a function of the length scale  $l_c$ . The points are obtained from simulations spanning the range  $0.01 \leq \phi \leq 0.9$  and  $0.001 \leq \alpha \leq 1$ . Concentrations are coded in color. The straight line corresponds to  $L_c = l_c$ . (b) Average stopping time  $T_{\text{stop}}$  as a function of  $\alpha$ . Points and color coding as in the left panel. Straight lines are power law fits for each concentration with exponent  $1.70 \pm 0.01$ . Inset: Data collapse plot against the time scale  $l_c^2/\alpha$ . The solid line is a power law fit with exponent 0.85 and the dashed line corresponds to exponent 1. (c) Distribution of stopping times  $S(t)$  (main figure) and overlap function divided by the SEP value (inset) for  $\phi = 0.5$  and  $\alpha = 0.005$ .

are exponentially distributed with a characteristic length scale  $L_c$ , which depends on  $\alpha$  and  $\phi$ . This dependence appears to be captured reasonably well by the length scale  $l_c = \sqrt{2\phi/[(1-\phi)\alpha]}$  that can be derived from a simple argument based on maximizing configuration entropy (see below), as the data collapse in Fig. 2a shows.

Since the clusters are immobile on the whole, the particles in the clusters will be stopped until they find a way to escape. When a moving particle joins a cluster it stops until it tumbles over a period of  $\alpha^{-1}$ . If new particles arrive during this period, the particle will be moved to the interior of the cluster and remain stopped for much longer times. We probe the statistics of the stopping times and find that they are widely distributed with a prominent tail at long times. The average stopping time, defined as  $T_{\text{stop}} = \sum_t tS(t)$  where  $S(t)$  is the average fraction of particles that have stopped for  $t$  time steps, is presented in Fig. 2b as a function of  $\alpha$  for different values of  $\phi$ . We observe a remarkable universal scaling behavior  $T_{\text{stop}} \sim \alpha^{-1.7}$  over 9 orders of magnitude in time. One might naively expect that the average stopping time is of the order of the time it takes for the cluster boundaries to diffuse (with the diffusion coefficient  $D_b$ ) across the cluster size  $l_c$ , namely,  $l_c^2/\alpha = 2\phi/[(1-\phi)\alpha^2]$ . Using this combination in fact does lead to data collapse for all relevant  $\alpha$  and  $\phi$  values (except for the region corresponding to large concentrations and large tumbling rates), as can be seen in the inset of Fig. 2b. However, the scaling plot has an effective exponent of 0.85, namely,  $T_{\text{stop}} \sim (l_c^2/\alpha)^{0.85}$ . This means that the effective motion of the boundary is in fact superdiffusive, presumably due to cooperative effects inside the clusters. The distribution of stopping times  $S(t)$  has an interesting behavior. For large  $\alpha$  it is dominated by particles with small stopping times, whereas for small  $\alpha$  it is bimodal as shown in Fig. 2c, revealing two distinct populations with small and large stopping times.

To further characterize the dynamics we also study the site-site temporal correlation or overlap function. At each site, we define  $s_i$  to be zero if the site is empty and one otherwise, regardless of the director of the particle. The overlap function is defined as

$$\Psi(t) = \frac{\langle s_i(t')s_i(t+t') \rangle - \phi^2}{\phi - \phi^2}, \quad (1)$$

which has been adequately normalized to give  $\Psi(0) = 1$  and vanish in the absence of correlations. The averaging is done over time  $t'$  and site position. The overlap function for the SEP has been computed exactly resulting in  $\Psi_{\text{SEP}} = e^{-t}I_0(t)$ , with the asymptotic large time expression  $\Psi_{\text{SEP}} \sim 1/\sqrt{2\pi t}$ , where  $I_n$  are the modified Bessel function of the first kind [13, 14]. Figure 2c (inset) shows the overlap function divided by  $\Psi_{\text{SEP}}$ , such that the effect of persistence in the dynamics can be probed. At intermediate times, we observe a large increase in the overlap as compared to the SEP. This enhanced overlap, that increases for decreasing  $\alpha$ , is due to the presence of jammed regions that trap particles for long times. At short times, the left and right borders of a given cluster perform independent random walks, and the overlap function exhibits an initial decay  $\Psi = 1 - (1-\phi)\sqrt{2\pi t}$ . At longer times, the clusters diffuse and the particles can perform a diffusive exclusion process, recovering the decay  $\Psi \sim 1/\sqrt{t}$ , albeit with a larger amplitude than the SEP as an effect of the retention time in the jammed regions. The crossover time between these two regimes,  $T_c$ , can be obtained numerically as the instant when  $\Psi/\Psi_{\text{SEP}}$  is maximum. We find the relation  $T_{\text{stop}} = 2T_c$  between the two time scales over the entire range of parameters studied, which shows that the two definitions are consistent and probe the same phenomenon.

At each time step, only a fraction  $\mu$  of the particles can move and the others are jammed. To understand the behavior of this quantity, which we call mobility, as

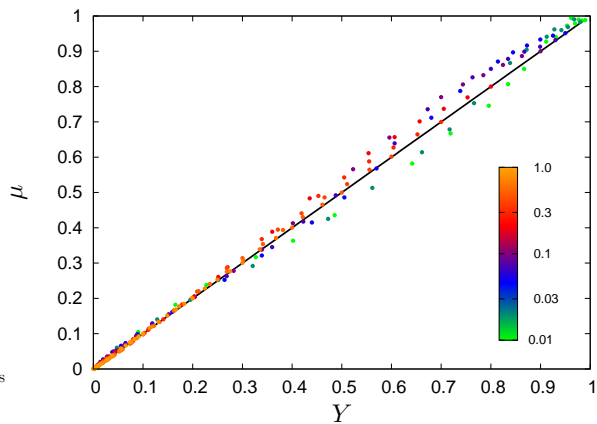


FIG. 3. (color online.) Representative data collapse plot for the fraction of moving particles  $\mu$  as a function of  $Y = \alpha(1 - \phi)(1 + \phi + 6\phi\alpha)/(\phi + \alpha + 6\phi\alpha)$ . Points and color coding as in Fig. 2. The straight line corresponds to  $\mu = Y$ .

a function of  $\phi$  and  $\alpha$ , it is helpful to examine its limiting forms. When  $\alpha \approx 1$ , we expect to obtain the SEP mobility  $\mu_{\text{SEP}} = 1 - \phi$ . It should decrease as  $\alpha$  is decreased, and vanish when  $\alpha = 0$ . When  $\phi$  is increased beyond  $\alpha$ , we expect the relative mobility to decrease  $\hat{\mu} = \mu/(1 - \phi)$ , due to the formation of the jammed regions. Other known exact asymptotic behaviors include  $\lim_{\alpha \rightarrow 1} \hat{\mu} = 1$ ,  $\lim_{\alpha \rightarrow 0} \hat{\mu} = 0$ , and  $\lim_{\phi \rightarrow 0} \hat{\mu} = 1$ . Note that the  $\phi = 0$  and  $\alpha = 0$  limits are singular and the behavior of the system depends on the order of these limits. The simulations show that  $\lim_{\phi \rightarrow 1} \hat{\mu}$  is a smooth function of  $\alpha$  that interpolates between 0 and 1. We find that it is possible to collapse our measured values of  $\mu$  versus  $\phi$  and  $\alpha$  using functions that interpolate smoothly between the above known asymptotic limits. Figure 2 shows one such collapse plot using a representative interpolation function

$$\mu \approx \frac{\alpha(1 - \phi)(1 + \phi + 6\phi\alpha)}{\phi + \alpha + 6\phi\alpha}. \quad (2)$$

We note that this mobility is the average value over the system where the clusters and the gas regions coexist, and it should not be confused with a mobility that depends on the local concentration [7, 8].

To obtain the exponential cluster size distribution, we consider each cluster to evolve independently of the others and construct a dynamic equilibrium that maximizes the configuration entropy subject to the relevant constraints. The total number of particles in the cluster phase,  $N_c$ , is fixed by the restriction that the concentration in the gas phase is  $\phi_g$ . This is imposed by a Lagrange multiplier  $\lambda$ , while a second multiplier  $\gamma$  is included to fix the total number of clusters  $C$ . Then, defining the number of clusters of size  $l$  as  $F_c(l)$ , we can construct the entropy as  $S = \log[C! / \prod_l F_c(l)!] - \lambda[N_c - \sum_l l F_c(l)] - \gamma[C - \sum_l F_c(l)]$ , which yields an exponential distribution  $F_c(l) = A_c e^{-l/\ell_c}$ . A similar reasoning allows us to derive the distribution of sizes in

the gas regions as  $F_g(l) = A_g e^{-l/\ell_g}$ . The constants  $A_c$ ,  $A_g$ ,  $\ell_c$ , and  $\ell_g$  can be fixed with the following prescriptions. (i) The average sizes are such that the total concentration is recovered:  $\langle l_c \rangle \phi_c + \langle l_g \rangle \phi_g = (\langle l_c \rangle + \langle l_g \rangle) \phi$ . (ii) The gas and cluster regions cover the entire system:  $\sum_l l F_c(l) + \sum_l l F_g(l) = N$ . (iii) There is equal number of gas and cluster regions:  $\sum_l F_g(l) = \sum_l F_c(l)$ . (iv) The dynamical balance in the number of dimers: Normally, the number of gas particles in each gas region is smaller than one, and the production of dimers is due to the emission in a time interval smaller than  $\ell_g$  of gas particles on the two sides of a gas region. Their production rate is then  $W_2^+ \approx \alpha(1 - e^{-\alpha\ell_g/2}) \sum_l F_g(l)$ . Their decay rate is simply due to evaporation with a rate  $W_2^- \approx \alpha F_c(2)$ . The final condition is then  $W_2^+ = W_2^-$ . Assuming that the cluster length scale  $\ell_c$  is large and approximating the sums by integrals, the transcendental equations can be solved to give  $\ell_c \approx \sqrt{2\phi/[(1 - \phi)\alpha]}$  and  $\ell_g \approx \sqrt{2(1 - \phi)/(\phi\alpha)}$ . Both length scales diverge when  $\alpha \rightarrow 0$ , and their behavior with the volume fraction is opposite, with  $\ell_c$  diverging at close packing.

The persistence exclusion process, which models hardcore run-and-tumble swimmers presents novel features that result from the collective dynamics. The steady state is characterized by the coexistence of jammed clusters and gas regions, which alternate. As a result of jamming, particles remain stopped for long times even at low global concentrations and only at much larger times diffusion is recovered. Clusters show an exponential stationary size distribution and there is no long scale coarsening. The jump between the jammed and gas regions is abrupt, rendering unsuitable the use of gradient expansions in coarse-grained descriptions. The predictions are in good quantitative agreement but power-law fits indicate that more complex cooperative effects should be considered to get a fully quantitative description of the dynamics, and in particular the counterintuitive universal superdiffusive escape of stopped swimmers in jammed regions.

This research is supported by Fondecyt Grant No. 1100100 and Anillo grant ACT 127 (R.S.), and Human Frontier Science Program (HFSP) grant RGP0061/2013 (R.G.).

- 
- [1] G. O'Toole, H.B. Kaplan, and R. Kolter, *Annu. Rev. Microbiol.* **54**, 49 (2000).
  - [2] P. Stoodley, K. Sauer, D.G. Davies, and J.W. Costerton, *Annu. Rev. Microbiol.* **56**, 187 (2002).
  - [3] P.K. Singh, A.L. Schaefer, M.R. Parsek, T.O. Moninger, M.J. Welsh, and E.P. Greenberg, *Nature* **407**, 762 (2000).
  - [4] M.L. Gibiansky, J.C. Conrad, F. Jin, V.D. Gordon, D.A. Motto, M.A. Mathewson, W.G. Stopka, D.C. Zelasko, J.D. Shrout, and G.C.L. Wong, *Science* **330**, 197 (2010); F. Jin, J. C. Conrad, M.L. Gibiansky, and G.C.L. Wong,

- Proc. Natl. Acad. Sci. USA **108**, 12617 (2011).
- [5] F. Peruani, A. Deutsch, and M. Bär, Phys. Rev. E **74**, 030904(R) (2006).
- [6] K. Kawasaki, A. Mochizuki, M. Matsushita, T. Umeda, and N. Shigesada, J. Theor. Biol. **188**, 177 (1997).
- [7] J. Tailleur and M.E. Cates, Phys. Rev. Lett. **100**, 218103 (2008).
- [8] A. Kudrolli, Phys. Rev. Lett. **104**, 088001 (2010).
- [9] F. Peruani, T. Klaus, A. Deutsch, and A. Voss-Boehme, Phys. Rev. Lett. **106**, 128101 (2011).
- [10] M.J. Schnitzer, Phys. Rev. E **48**, 2553 (1993).
- [11] Y. Kafri and R.A. da Silveira, Phys. Rev. Lett. **100**, 238101 (2008).
- [12] A.G. Thompson, J. Tailleur, M.E. Cates, and R.A. Blythe, J. Stat. Mech. P02029 (2011).
- [13] D.L. Huber, Phys. Rev. B **15**, 533 (1977).
- [14] P.M. Richards, Phys. Rev. B **16**, 1393 (1977).
- [15] T.M. Liggett, *Interacting Particle Systems* (Springer-Verlag, New York, 1985).
- [16] B. Derrida, Phys. Rep. **301**, 65 (1998).
- [17] B. Derrida, S.A. Janowsky, J.L. Lebowitz, and E.R. Speer, J. Stat. Phys. **73**, 813 (1993).
- [18] T. Chou, K. Mallick, and R. K. P. Zia, Rep. Prog. Phys. **74**, 116601 (2011).
- [19] M. Gorissen, A. Lazarescu, K. Mallick, and C. Vanderzande, Phys. Rev. Lett. **109**, 170601 (2012).
- [20] I. Neri, N. Kern, and A. Parmeggiani, Phys. Rev. Lett. **107**, 068702 (2011).
- [21] H.C. Berg, *E. coli in Motion* (Springer-Verlag, New York, 2004).